Assessment of Density and Character of Dislocations in Cyclic Loaded Stainless Steel Using X-ray Diffraction Profile Analysis

A thesis submitted in partial fulfillment of the

requirement for the degree of

Master of Technology

in

Metallurgical and Materials Engineering

by

Rajat Kishor

Roll no: 212MM1415

Department of Metallurgical and Materials Engineering
National Institute of Technology, Rourkela

May 2014

Assessment of Density and Character of Dislocations in Cyclic Loaded Stainless Steel Using X-ray Diffraction Profile Analysis

A thesis submitted in partial fulfillment of the

requirement for the degree of

Master of Technology

in

Metallurgical and Materials Engineering

by

Rajat Kishor

Under the guidance of

Prof. Ashok Kumar Mondal

Department of Metallurgical and Materials Engineering

National Institute of Technology, Rourkela

May 2014

National Institute of Technology, Rourkela

Certificate

This is to certify that the thesis entitled, "***Assessment of Density and Character of Dislocations in Cyclic Loaded Stainless Steel Using X-ray Diffraction Profile Analysis"*** submitted by **Mr. Rajat Kishor** in partial fulfillment of the requirements for the award of the degree of **Master of Technology** in **Metallurgical and Materials Engineering** at the **National Institute of Technology, Rourkela** is an authentic work carried out by him under my supervision and guidance.

To the best of my knowledge, the matter embodied in the thesis has not been submitted to any other University/ Institute for the award of any degree or diploma.

Date: **Supervisor**

Place: Rourkela **Prof. A. K. Mondal**

Department of Metallurgical
and Materials Engineering
National institute of Technology,
Rourkela-769008

Acknowledgement

I would like to express my deep sense of gratitude and respect to my supervisor **Prof. A. K. Mondal**, Metallurgical and Materials Engineering Department, NIT Rourkela, for his inspiring guidance, constructive criticism and valuable suggestions throughout the research work. It would have not been possible for me to bring out this thesis without his help and constant encouragement.

I am sincerely thankful to Prof. **K. Dutta**, Metallurgical and Materials Engineering for his persistent support and advice during the course work.

I am also highly grateful to other members of Department of Metallurgical and Materials Engineering, NIT Rourkela, specially Prof. S.K. Sahu, for his help during execution of experiment.

I am thankful to all my classmates and friends who made my stay in Rourkela, an unforgettable and rewarding experience.

Finally, I feel great reverence for all my family members and the Almighty, for their blessings and for being a constant source of encouragement.

Place: Rourkela **Rajat Kishor**

DEDICATED TO MY PARENTS AND GOD

CONTENT

CHAPTER 4 **RESULTS AND DISCUSSION**

CHAPTER 5 **CONCLUSIONS**

Abstract

Asymmetric stress-controlled fatigue i.e., ratcheting behaviour of a non-conventional stainless steel X12CrMnNiN17-7-5 has been investigated with varying mean stresses, stress amplitudes and number of cycles at room temperature using a servo hydraulic universal testing machine. The X-ray diffraction profile analysis using the modified Williamson–Hall equation has been carried out in order to estimate the dislocation densities in the specimens subjected to ratcheting deformation. Increase in strain accumulation has been explained by increase in dislocation densities in the ratcheted specimens and a correlation between the strain produced by ratcheting deformation and the estimated dislocation density has been established.

LIST OF FIGURES

LIST OF TABLES:

CHAPTER 1

INTRODUCTION

1. Introduction:

1.1 Description and background

Stainless steels are the candidate material for applications in chemical, process and power generation industries owing to its excellent combination of mechanical properties, oxidation and corrosion resistance under monotonic and cyclic loading conditions [1]. Amongst the numerous grades of stainless steels, the austenitic stainless steels are class of materials having face centred cubic lattice structure which is stable from room temperature to the melting point. X12CrMnNiN17-7-5 (ISO/TR 15510) is a non-conventional special grade of austenitic stainless steel that was developed to conserve Ni and is potentially used for making components such as trim, wheel covers, flat conveyer chains, railroad passenger car bodies etc. The steel is used in architectural applications such as doors, panels, window and frame. In such applications, deformation of the components is primarily dictated by various kinds of fatigue like high and low cycle fatigue, asymmetric stress-controlled fatigue etc. The asymmetric stress-controlled fatigue (also known as ratcheting) takes place when components deform under the influence of positive or negative mean stress (σ_m) by accumulating positive or negative plastic strain (ϵ_p) in the structure, respectively. Therefore, it is a critical issue and emphasis must be laid to understand the ratcheting behaviour of the X12CrMnNiN17-7-5 stainless steel.

It is established that stainless steels undergo phase transformation upon deformation [2,3] and the same is expected to take place in this steel as well. The ratcheting deformation of materials takes place owing to the variations in microstructures and the dislocation density in it during the course of load application. However, the number of literature relating the microstructural variations and the dislocation density with the strain accumulation during ratcheting deformation

is limited. In addition, the ratcheting behaviour varies with the applied mean stresses (σ_m), stress amplitudes (σ_a) and number of cycles (N) since the microstructures and the dislocation densities in the specimens change with these. Therefore, the estimation of dislocation densities in the microstructures of the tested specimens in each condition would be of immense importance to provide a clear picture of the extent of deformation induced in the specimens. In recent years it has been reported in literature that accumulation of ratcheting strain can be correlated with dislocation activity of the material and increased strain accumulation takes place under increased cyclic loading parameters, with increased dislocation densities in ratcheted samples.

Dislocation density in cyclically deformed materials can be measured by direct methods like Transmission Electron Microscopy (TEM) and indirect methods like X-ray or neutron diffraction [4-6]. The direct methods reveal the microstructural information in an extremely small area of specimen, whereas the indirect methods reveal the average data over a relatively large area exposed to irradiation. The preparation of specimen for TEM study is difficult and complicated. In addition, the thinness of TEM specimen sometimes results in a low dislocation density [7]. On the contrary, the specimen preparation for studying X-ray diffraction is easy and less time consuming. In addition, the tests can be performed over a bulk specimen that is suitable for estimating dislocation density of a material more precisely. Accordingly, X-ray diffraction profile analysis is used for various specimens such as bulk single and polycrystalline materials; polycrystalline powders and single phase materials to reveal various information such as dislocation density, dislocation character and crystal size [8-10].

In the present investigation, asymmetric stress-controlled fatigue (ratcheting) behaviour of a non-conventional stainless steel has been studied with varying mean stresses (σ_m), stress amplitudes (σ_a) and number of cycles (N). The X-ray diffraction profile analysis has been carried out in order to estimate the dislocation densities in the specimens subjected to ratcheting deformation and a correlation between the strain produced by ratcheting and the estimated dislocation density has been established.

Ungar et.al, Gubicza et.as, Dragomir et.al, Renzetti et. al have studied the dislocation character in copper, polycrystals, titanium, ODS-Eurofer steel under tensile deformation, extrusion, hot rolling, cold roll conditions respectively. But no earlier investigation exists in literature for the character of dislocations in ratcheted stainless steel. Hence an attempt has been made to assess and estimate the dislocation character and respective densities in asymmetrically fatigue cycled non conventional stainless steel.

1.1 Objectives of the work:

(i). Calculating dislocation density by XRD profile analysis:

Previously dislocation density was calculated with the help of Transmission Electron Microscopy (TEM) which is a typical job and it takes too much time so to calculate dislocation density XRD profile analysis is an easy approach as compared to TEM. It takes much less time and provides accurate results.

(ii). Correlating ratcheting strain and dislocation density (DD) by XRD:

Due to low cycle fatigue load ratcheting strain develops in the specimen due to which dislocation occurs. In the present work a relation between ratcheting strain and dislocation density is shown and their dependency on each other is provided.

(iii). Calculation of dislocation density in each phase:

Due to load applied phase transformation occurs in the material. The value of dislocation density never remains constant throughout each phase. So in the present work dislocation density in each phase is calculated separately.

(iv). Comparison between edge and screw dislocation:

Two types of dislocation were found in the specimen and those were edge and screw dislocation. In the present work both dislocations were calculated and a comparison is provided between these two dislocations in each phase.

The thesis has been divided into five chapters. **Chapter-1** deals with the details of non conventional stainless steel and its applications in the field engineering. **Chaper-2** is provided with a detailed literature review and past history of the work. **Chapter-3** deals with the quantitative and qualitative analysis of the specimen used in present calculations. **Chapter-4** Covers all the result and possible correlation for the investigation. **Chapter-5** Deals with summary and conclusions for present work. References cited are enlisted after chapter-5.

CHAPTER 2

LITERATURE REVIEW

2.1 Introduction of stainless steel:

Stainless steel is also known as inox steel in metallurgical field. It contains a minimum of 10.5% chromium mass. Because of having some vast properties like non corrosive, non rusting or non staining with water as ordinary steel does, stainless steel is mostly used. But it loses some of its properties under less oxygen content, or poor flow environments. That is why there are several different grades of stainless steel according to the environment the alloy must endure.

By the amount of chromium present in the alloy stainless steel differs from carbon steel. Unprotected carbon steel rusts readily when exposed to air and moisture. A film of iron oxide appears on the steel and this only hastens the corrosion by the formation of more and more oxide on the surface, and due to this more amount of oxide formation it tends to flake and fall away. This type of corrosion is prevented by stainless steel due to chromium which forms a passive film of chromium oxide. Due to which oxygen gets blocked and can not be diffused to steel and thus blocks corrosion on to the surface. It has one more benefit that the size of steel and oxide ions is similar so they remain attached to the surface. [11]

2.1.1 Properties of Stainless steel:

(i) Oxidation:

High resistance to oxidation at normal atmospheric temperature is generally attained with minimum addition of 13% chromium (weight), till 26% used for harsher environments. When chromium is exposed with oxygen it forms a passive layer of oxide of chromium (III) i.e. (Cr_2O_3). The Cr_2O_3 layer is thin and invisible, and the stainless steel metal relics flexible and

lustrous. Passive layer is impermeable into H_2O and ambient air which protects the required metal underneath, and if the surface gets scratched this layer reforms itself quickly. This occurrence is known as passivation and is also seen in aluminum and sometimes in titanium. Resistance to corrosion can be negatively affected if the constituent is used in an environment consisting of no oxygen, typical example would be submerged keel bolts masked in wood.

When metal components like nuts are enforced together with bolts, the layer gets scraped off, which allows the parts to join. If effectively disassembled, the part which is welded might be torn and gnarled, and this effect is identified as galling. Use of unlike resources for the components enforced together can avoid galling, for instance bronze or even various kinds of stainless steels (which is martensite alongside austenite). Though, two varied alloys linked electrically in a atmosphere contain humidity can operate as voltaic pile and rust quicker.

(ii) Acids:

Stainless steel is usually non favorable to acid, however this characteristic is dependent on the type and the amount of concentration of the particular acid, immediate temperature, and type of steel. At room temperature and high concentrations sulfuric acid does not corrode Type 304, but in low concentrations type 316,317 gets corroded. Nitric acid has been used successfully for all sorts of stainless steel resistance attacks from attack of phosphorous, 316,317 more than 304 and also Types 304L, 430. Hydrochloric Acid can damage stainless steel of any type, and must be evaded.

(iii) Bases:

The three hundred chain of stainless steel grade is unchanged by feeble bases like hydroxide of ammonia, even at elevated atmospheric temperatures and in soaring concentration. The similar

grade of stainless steel bare to strong bases like sodium hydroxide in elevated temperatures and enough concentrations will be having some etch, particularly to the solutions which contain chlorides.

(v) Electricity and magnetism:

Stainless steel conducts electricity moderately same as steel, containing less percentage of copper's electrical conductivity. Ferritic and martensitic are magnetic stainless steels. Austenitic is a non-magnetic stainless steel.

2.1.2 Applications:

It is a perfect material for various applications as it is both rust and staining resistive, also low maintenance and has a recognizable luster. Stainless steel has more than 150 grades, out of them fifteen are mainly used. Stainless steel is milled in various forms such as coil, sheet, plate, bar, cable and tubes which are used in household cookware, crockery, hardware, surgical equipments, factory equipment(for instance, in sugar mills and like an automobile and aerospace structured alloy and production material in big buildings. This also affects its utility in kitchens and food processing units, as they can be cleaned with steam and sterilized and do not require paint or other exterior finishes. 316L is the type mainly used for making jewelry and watches. Few numbers of automotive manufacturers make use of stainless steel as ornamental attractions in their vehicle.

2.2. Fatigue:

2.2.1 General concept:

Due to regularly applied load there is a weakening of materials occur which is termed as fatigue in the field of materials. When a material is under cyclic loading of any kind there is progressive and localized structural damage in the material can be seen. The value of maximum stress due to which such damage occurs is much less than the ultimate tensile strength limit or yield stress limit of the material.

When the load reaches maximum threshold microscopic cracks start forming at the stress concentrators which are surface, persistent slip bands (PSBs). After some time the crack will reach to a critical size and starts propagating due to which fracture in the structure occurs. Shape of the structure plays a vital role in crack propagation as affects fatigue life like square holes or sharp corners are the place which leads to elevated local stresses and at that places fatigue cracks can initiate more rapidly.

2.2.2 Fatigue life:

According to ASTM fatigue life (N_f) can be defined as the capacity of material that can sustain several numbers of stress cycles having a particular character before failure.

The best method which can dictate fatigue life is Uniform Material Law (UML). Initially it was investigated for the forecasting of fatigue life of aluminum alloy and titanium alloys and then it was extended to the steels having higher strength. There is a value of stress amplitude and lower to that value the material will never undergo and kind of failure which is termed as fatigue limit or endurance limit.

2.2.3 High Cycle Fatigue:

Previously the aim was to focus on the situation which required 10^4 cycles to get failed and there stress value was very less due to which the deformation occurred was elastic.

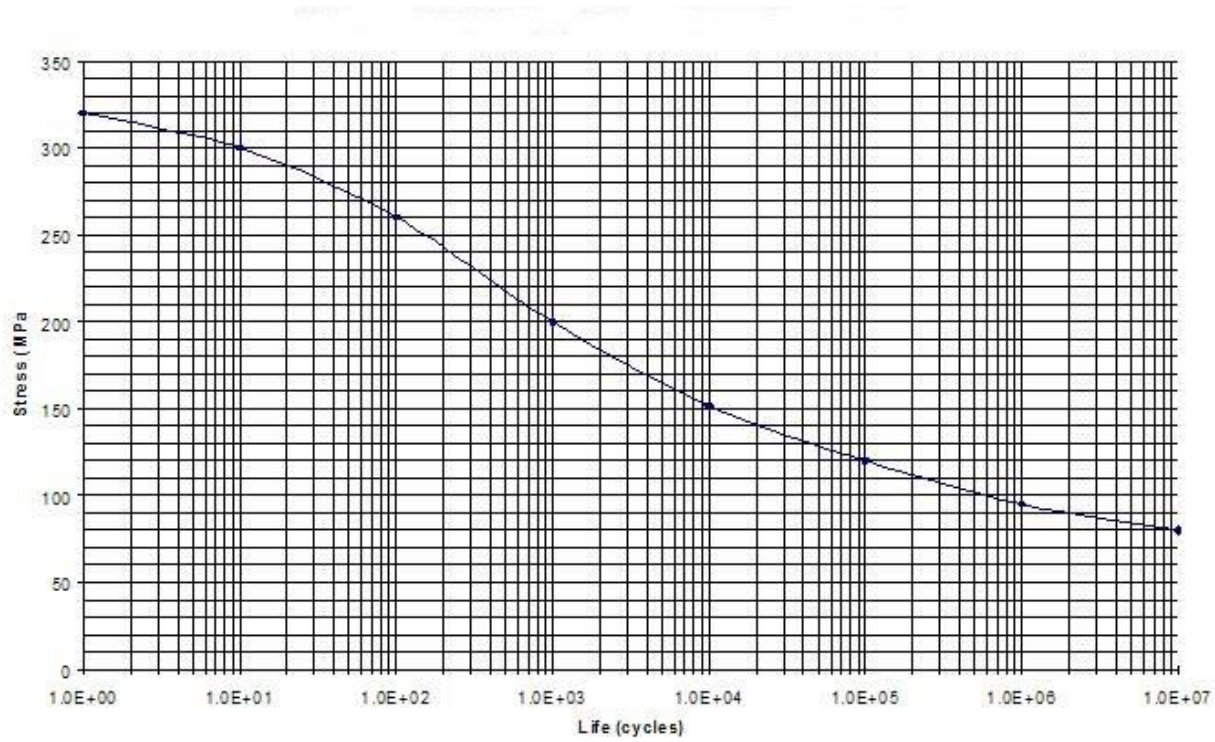

Fig 2.1 S-N curve for brittle Al with ultimate tensile strength of 320 Mpa

There is a simple way to derive S-N curves from the samples of the related material which are also known as coupons is to apply a frequent sinusoidal stress by the testing machine. This testing machine can also detect the number of cycle on which the material is failed. This procedure is also termed as coupon testing. A point on the plot is generated on every test even if in some special conditions some kind of run out occur which delays the failure time which is

presented for the test. Fatigue data is analyzed with the help of some methods that needs statistics and among them survival analysis & linear regression is important.

Several factors affect the succession of S-N plot out of those corrosion, residual stress, notches are main. Mean stress persuades the fatigue strength in a broad way which can be authorized by Goodman-Line.

2.2.4 Low cycle fatigue:

In some cases where plastic deformation can occur due to high stress, strain provides an uncomplicated and perfect depiction rather than stress. Coffin-Manson proposed a relationship for the characterization of low cycled fatigue

$$\frac{\Delta\epsilon_p}{2} = \epsilon'_f(2N)^c$$

Where:

- $\Delta\varepsilon_p$ /2 is strain amplitude in plastic condition.
- ε_f' is a constant which is termed as fatigue ductility coefficient.
- c is a constant varies from -0.5 to -0.7 in case of metals and termed as fatigue ductility exponent.

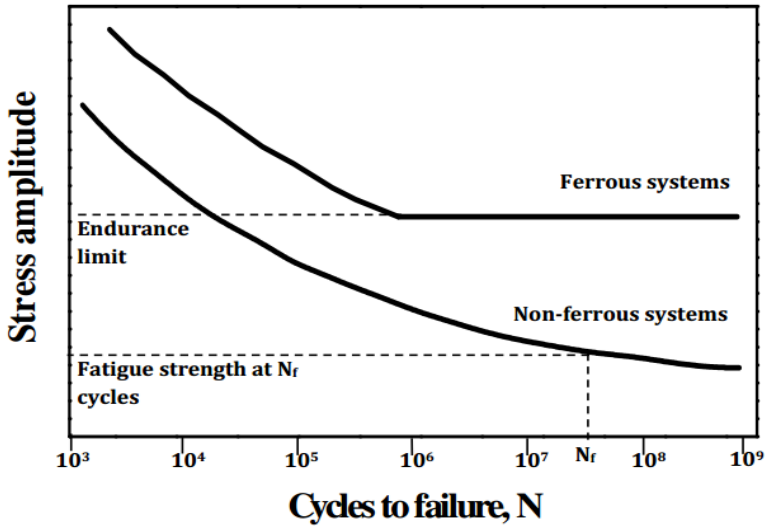

Fig. 2.2 Representation of ferrous and non-ferrous system S-N curve

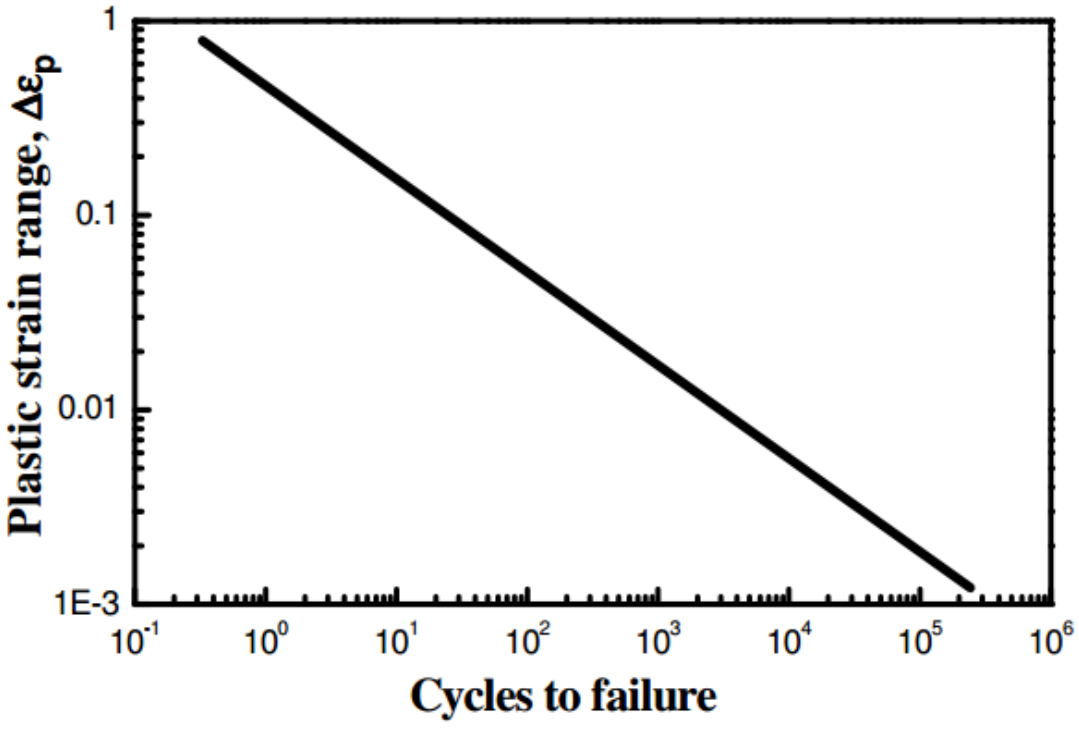

Fig. 2.3 Representation of fatigue curve for low cycle

2.3 Ratcheting phenomenon and its description:

Ratcheting is a kind of strain which occurs when low cycle fatigue is employed to the specimen i.e cyclic loading in asymmetrical condition is applied. Hysteresis loops are formed for each loading cycle. Hysteresis loop thus generated turns in the direction of high plastic strain for consequent cycles [13].

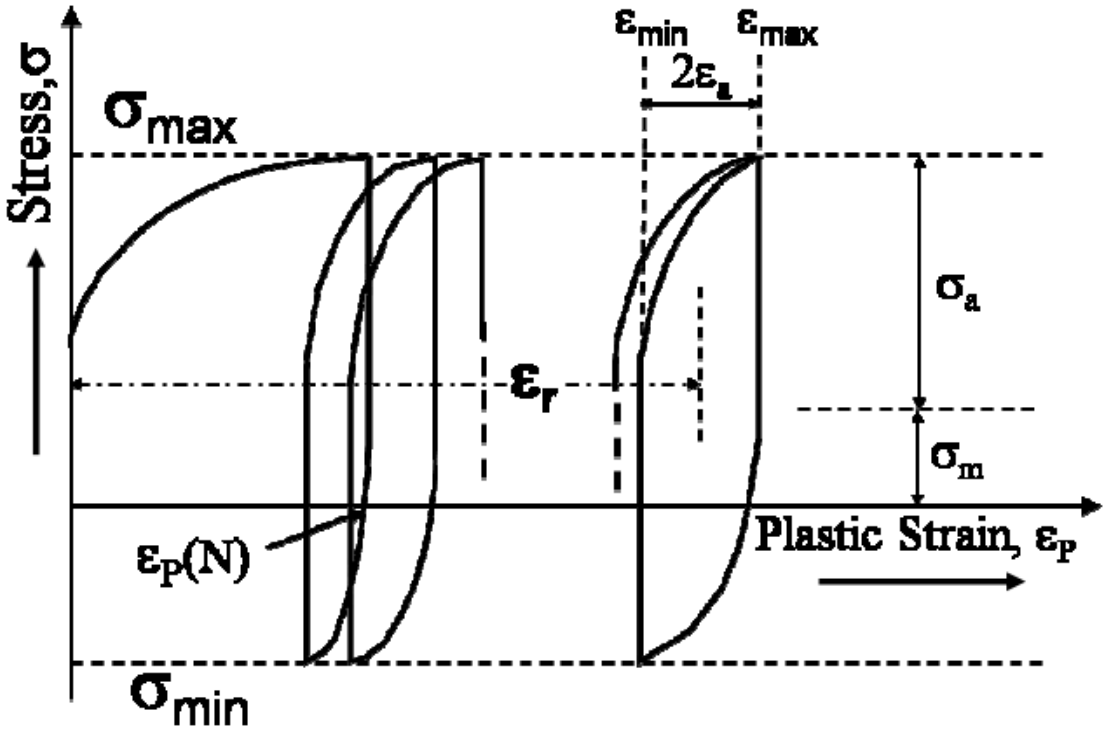

Fig. 2.4 schematic presentation of hysteresis loop and shifts.

Here, σ_{max} = Max. stress, σ_{min} = Min. stress, σ_m = Mean stress, σ_a = Stress amplitude

Ringsberg has explained the phenomenon as those cases where there is some added plastic deformation for each and every cycle of loading is termed as ratcheting. In such cases accretion of strain is prolonged until ductility of material is vanished and the material comes to rupture condition. There is a continuous decrement in the rate of strain accumulation with each increment in no. of cycle which indicates that the material is going towards steady state.

The measurement of ratcheting cycle can easily be provided in terms of mean strain in a specific number of cycle and can be expressed as:

$$\varepsilon_r = (\varepsilon_{max} + \varepsilon_{min})/2$$

Where, ε_r is the axial ratcheting strain

ε_{max} is the value of maximum strain for a particular cycle

ε_{min} is the value of minimum strain for that cycle.

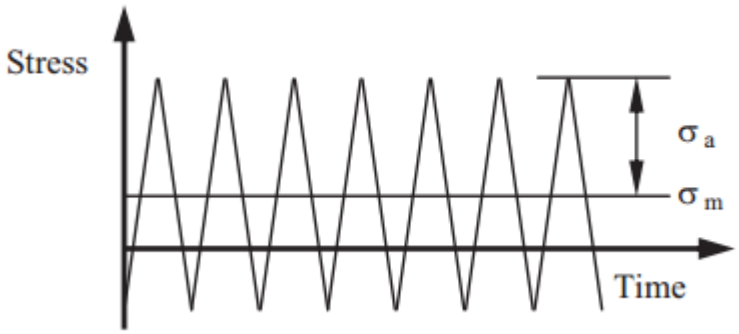

Fig.2.5 schematic loading path for ratcheting test.

Ratcheting strain provides an important tool for designing and evaluating the life of various structural component used in cyclic loading. There are various kinds of components which

are used in cyclic loading condition and their stress value is more than the elasticity of that material. Because of ratcheting structures are subjected to catastrophic failure so in these kinds of materials accurate prophecy of ratcheting is critical from design point of view. As the number of cycles increase ratcheting strain (Ɛr) also increases constantly and due to which there is a plastic strain accretion with time ad causes material to fail. If ratcheting strain (Ɛr) becomes constant after increasing initially with number of cycles it shows that only in the first section of curve plastic strain accumulates and then it stops in constant ratcheting strain region hence it prevents material to fail. [14]

2.3.1 Parameters effecting strain accumulation during ratcheting:

Several parameters are there which affects the strain accumulation because of ratcheting. Type of loading which shows how load is applied to the material is the main parameter which effects the strain accumulation in case of asymmetric cyclic loading. Types of loading can be précised as mean stress, stress amplitude, maximum stress, stress rate, stress ratio, cyclic hardening and cyclic softening behavior.

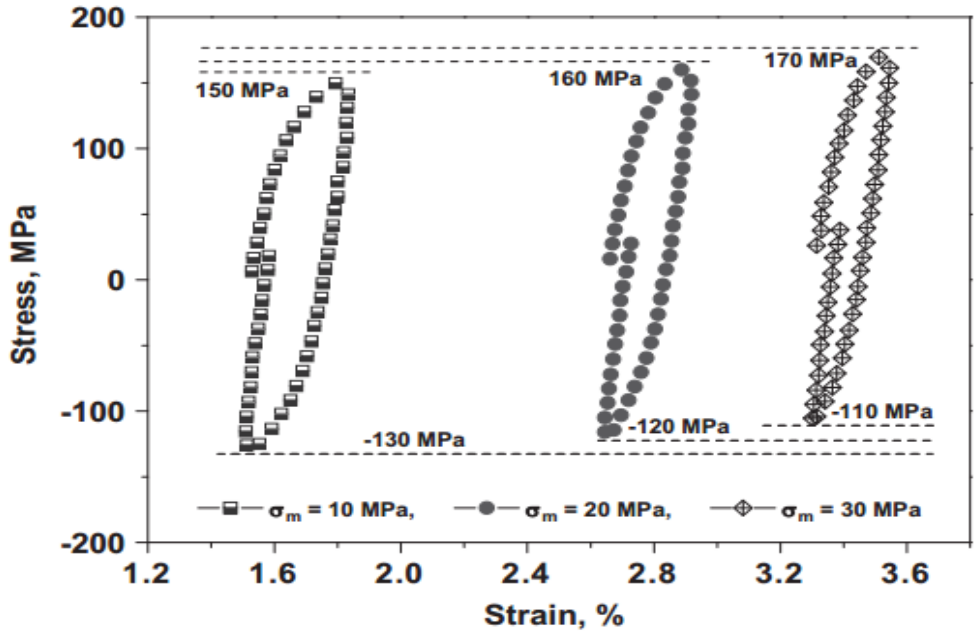

Fig.2.6 Stress–strain hysteresis loops (N=10) showing variations in their relative positions.

2.4 Dislocation:

In the field of material science dislocation is a defect in crystal structure or we can also say it as irregularity in crystal structure. Due to the dislocation many properties of the material get influenced. Initially the theory which describes the defects occur in elastic field was proposed by Vito Volterra in 1907, dislocation the exact term which refers to defect on atomic level was proposed by G. Taylor in the year of 1934 [15]. In some cases dislocation can be envisaged as occurred due to shifting of a plane at the middle of crystal structure. In these cases the planes which surround them does not remain straight and they bend itself around the corner of the terminating plane. Because of this the structure of the crystal remains perfectly ordered on either side. In can be analyzed by a analogy that if half portion of a paper is inserted in stack of papers the defect can only be seen at the edge.

Mainly there are two types of dislocation, first is edge dislocation and other is screw dislocation. Mixed dislocations are also a kind of dislocation which falls between these two. Dislocations are also known as Soliton and it can be said as a topological defect mathematically. Mathematics explains why the behavior of dislocation is like stable particles as dislocations remain their identity while moving also. Dislocations of reverse orientation have the property that they can cancel their selves but a single dislocation will remain its identity and will not disappear by its own.

2.4.1 Edge dislocations:

The edge dislocation can be said to occur when atoms of extra plane is introduced in the mid of the crystal and because of that nearby atoms of different plane is distorted. This extra plane crosses through the other planes of atom when sufficient force is given to one side and it breaks and joins bond with them until grain boundary is reached. Form fig. 2.7 concept of extra plane can be illustrated and can be termed as dislocation. The major criteria to define the edge dislocation is Burgers vector which provides the magnitude as well as direction of dislocation and in case of edge dislocation Burgers vector is perpendicular to the line direction.

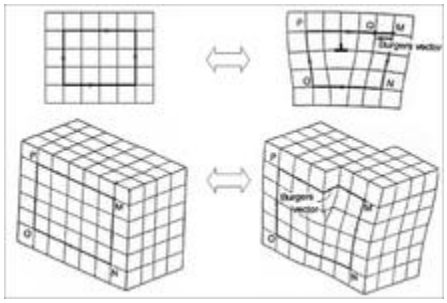

Fig. 2.7 Schematic representation of edge dislocation.

2.4.2 Screw dislocations:

It is too tough to visualize screw dislocation. Suppose a cutting of crystal through a plane and by a lattice vector slip one half of it across the other, the halves fitting back together and any defect will not be left. If the cut only goes part way through the crystal, and then slipped, the boundary of the cut is a screw dislocation. Like edge dislocation screw dislocation can also be identified by Burgers vector and in this case it will move parallel to the direction.

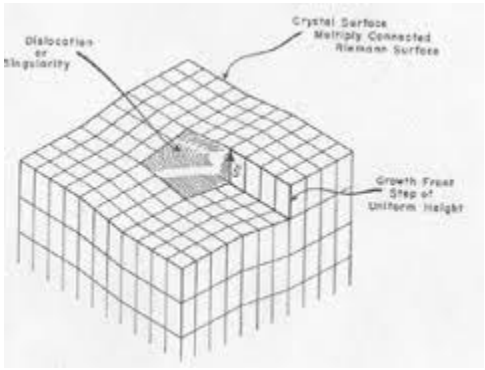

Fig. 2.8 Schematic representation of screw dislocation.

The stress generated due to screw dislocation is less difficult than edge dislocation and it can be calculated by using one simple equation because it allows only single radial coordinate to use. The equation is as follows:

$$\tau_r = \frac{-\mu b}{2\pi r}$$

where μ is the shear modulus of the material, b is the Burgers vector, and r is a radial coordinate.

2.4.3 Calculation of dislocation density:

Dislocation density in cyclically deformed materials can be measured by direct methods like Transmission Electron Microscopy (TEM) and indirect methods like X-ray or neutron diffraction [4-6]. The direct methods reveal the microstructural information in an extremely small area of specimen, whereas the indirect methods reveal the average data over a relatively large area exposed to irradiation. The preparation of specimen for TEM study is difficult and complicated. In addition, the thinness of TEM specimen sometimes results in a low dislocation density [7]. On the contrary, the specimen preparation for studying X-ray diffraction is easy and less time consuming. In addition, the tests can be performed over a bulk specimen that is suitable for estimating dislocation density of a material more precisely. Accordingly, X-ray diffraction profile analysis is used for various specimens such as bulk single and polycrystalline materials; polycrystalline powders and single phase materials to reveal various information such as dislocation density, dislocation character and crystal size [8-10].

CHAPTER 3

QUANTITATIVE AND QUALITATIVE ANALYSIS

3.1 Estimation of dislocation density:

- For this evaluation the specimens chosen were already experimented. It wass a commercially pure non-conventional austenitic stainless steel which is known as X12CrMnNiN17-7-5 according to ISO/TR 15510:1997 [16]. The material was procured in the form of a round bar having diameter of 16 mm. The past history of the steel was not known and therefore, it was required to remove any residual stresses present in it. The steel was further subjected to solution annealing that helped in dissolving carbide phases at high temperature. The solution annealing of the steel was carried out by heating the steel at 960°C for 1 hr followed by water quenching. The specimens for microstructural analysis were mechanically polished up to 0.25 µm surface finish and they were electro polished using a solution of 20% perchloric acid and 80% acetic acid in ice-cooled atmosphere. The polished specimens were etched with aqua regia a solution of 75% HCl and 25% HNO_3.
- XRD profile was taken for all kinds of analysis.
- The X-ray scan parameters used are as follows:
  - Scanning angle: 40^0 to 120^0 of 2.
  - Step size for scanning: 2 deg.
  - Time per step: 1 minute.

The modified Williamson–Hall equation [17] is employed in order to calculate the dislocation densities in the austenite (γ) and martensite (α′) phases in the stainless steel under investigation at room temperature. Assuming that the strain broadening is caused owing to the presence of the dislocations generated during the ratcheting deformation, the full width at half maximum (FWHM) of diffraction profiles can be expressed by the modified Williamson–Hall plot as [17]

$$\Delta K \cong 1/d + \left(\frac{\pi M^2 b^2}{2}\right)\rho^{1/2}\left(K^2\overline{C}\right) + O\left(K^4\overline{C}^2\right)$$

Where $K = 2\sin\theta/\lambda$,

$\Delta K = \cos\theta(\Delta 2\theta)/\lambda$

θ is the diffraction angle,

$\Delta(2\theta)$ is the integral breadth (FWHM) of the diffraction peak,

λ is the wavelength of the X-rays,

d is the average grain size,

b is the length of the Burgers vector of the dislocations,

and ρ is the average dislocation density.

M is a constant depending on both the effective outer cut-off radius of dislocations and the dislocation density. The value of M varies in between 1 and 2 for deformed materials [18,19]. Following this proposition, the value of M = 2 is used for all the specimens subjected to ratcheting deformation in the present investigation.

The value of C represents the average contrast factor of the dislocations for a particular reflection. The average contrast factor for different diffraction vectors are defined as:

$$C = C_{h00}\left[1 - q\left(\frac{h^2k^2 + k^2l^2 + l^2h^2}{h^2 + k^2 + l^2}\right)\right]$$

Where C_{h00} is the average contrast factor corresponding to h00 reflection. The value of $C_{h00} = 0.266$ is obtained from Ungár et al. [20]. The value of q = 2.203 is calculated based on the expression provided in Ungár et al. [20]. O indicates non-interpreted higher order terms in $K^4\overline{C}^2$ and therefore, the term containing it is ignored.

3.2 Calculation of Dislocation Character:

Dislocation character implies that there is separate dislocation viz. edge and screw in each phase. So the value of 'C' which we have taken as an average value for all type of dislocations will not be considered here. Ungar et. al has provided the way to calculate the value of 'C' in each phase.

3.2.1 The value of $\bar{C}_{h00}$ in FCC and BCC crystals:

Calculation of average values of the contrast factors were done for the most common slip systems in the FCC and BCC systems. Value of $\bar{C}_{h00}$ in both cases like edge and screw were evaluated by arithmetic averages of the individual C_{h00} values and these are the functions of A_i and C_{12}/C_{44}. No dependence on c_{12}/c_{44} was seen for screw dislocations in case of f.c.c. crystals, while in case of edge dislocations, a comparatively strong dependence on c_{12}/c_{44} was observed. The A_i dependence of $\bar{C}_{h00}$ at different c_{12}/c_{44} values can be parameterized by the following function:

$$\bar{C} = a[1-\exp(-A_i/b)] + cA_i + d$$

Where a,b,c,d are constants and their corresponding values are given in table 4.2.

3.2.2 The values of q in FCC and BCC crystals:

In the range between 0.5 and 3 q is found to be independent of C_{12}/C_{44} for screw dislocations (at least in f.c.c. crystals). In case of edge dislocations, q shows a weak dependency on C_{12}/C_{44} in the range of 0.5 to 1, while in between 1 and 3 this dependency becomes trivial. The A_i dependence of q at different c_{12}/c_{44} values can be characterized by the same kind of equation as

$$q = a[1-\exp(-A_i/b)] + cA_i + d$$

The values of a, b, c, d for FCC as well as BCC are listed in Table 4.3. Large difference can be found, especially in the range of 0.5 and 4 for A_i.

CHAPTER 4

RESULT AND DISCUSSION

4. Results and discussion

4.1. Microstructure

A typical micrograph of the stainless steel under investigation is shown in Fig. 4.1. It is evident from the figure that the steel possesses equi-axed austenite grains. The grain size was measured using linear intercept method as per ASTM E112 standard and the same was 65±4.3 µm.

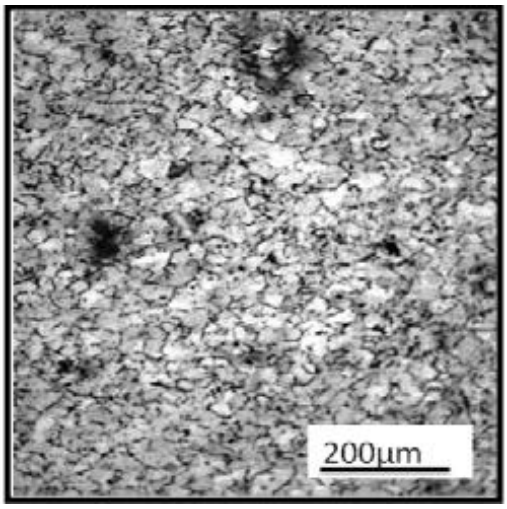

Fig. 4.1: A typical optical micrograph of the investigated non-conventional stainless steel.

4.2. Accumulation of ratcheting strain

The accumulation of ratcheting strain attains a saturation plateau after about 100 cycles of loading for stainless steels [21]. Therefore, the first set of ratcheting tests was carried out up to 100 cycles of loading and another set of tests was carried out up to 50 cycles of loading for comparison. Typical set of hysteresis loops produced during ratcheting deformation is shown in Fig. 4.2 for σ_m-σ_a combination of 150 and 500 MPa. It is evident from the figure that the accumulation of ratcheting strain produces unclosed hysteresis loops which shift towards positive plastic strain with increase in number of cycles, as the applied mean stress is positive, as expected. It is available in literature that hysteresis loops shift towards negative plastic strain when the applied mean stress is negative [22]. The variation of ratcheting strain with mean stresses (σ_m), stress amplitudes (σ_a) and number of cycles (N) employed in the present investigation is shown in Fig. 4.5 (a&b). It can be seen from these figures that accumulation of ratcheting strain increases with increase in mean stress (σ_m) at constant stress amplitude (σ_a) and number of cycles (N); with increase in stress amplitude (σ_a) at constant mean stress (σ_m) and number of cycles (N) as well as with increase in number of cycles (N) at a constant mean stress (σ_m) and stress amplitude (σ_a). When σ_m increases at a constant σ_a total zone of fatigue cycling shifts towards more positive side with an increase in applied maximum stress at the particular condition and therefore, strain accumulation increases. The increment in strain accumulation can also be explained using plastic strain amplitude ($\Delta\varepsilon_p$) approach. The accumulation of ratcheting strain increases due to increase in the opening of hysteresis loops when σ_a is increased at constant σ_m. This increases $\Delta\varepsilon_p$ at a particular cycle, i.e., strain accumulation increases [23].

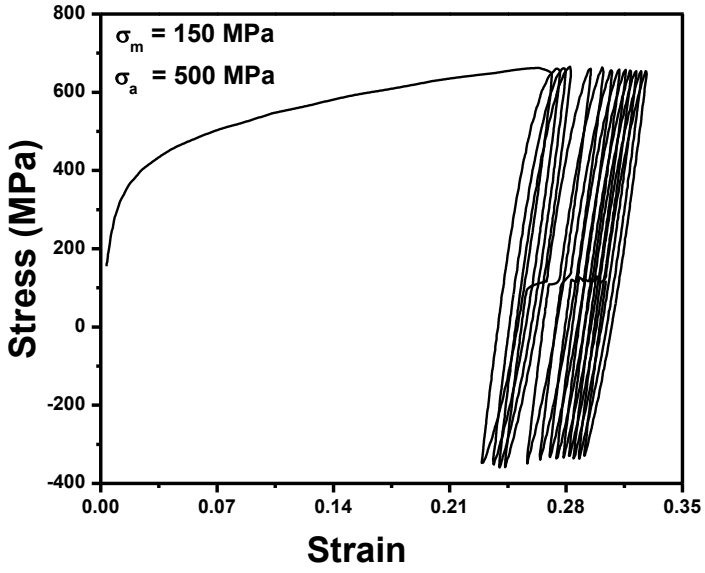

Fig. 4.2: A typical set of hysteresis loops generated during ratcheting deformation for σ_m- σ_a combination of 150 and 500 MPa.

The accumulation of ratcheting strain, till now has been discussed from mechanistic point of view. However, material's substructure varies owing to ratcheting deformation as well. The accumulation of ratcheting strain is dictated by the evolution of dislocation characteristics in the substructure in material [21]. Transmission electron microscopy is the most suitable tool to visualize the substructural features in materials; however, the potential of X-ray diffraction profile analysis is realized only recently. Variations in dislocation densities in the ratcheted specimens have been estimated using X-ray diffraction profile analysis; the results and corresponding discussion have been substantiated in section 4.4.

Table 4.1Test matrix used for all ratcheting experiments (same for 50 and 100 cycles of loading).

Mean stress (σ_m), MPa	Stress amplitude (σ_a), MPa
100	400
	450
	500
150	400
	450
	500
200	400
	450
	500

4.3. Phase transformation during ratcheting deformation

The XRD patterns obtained from the as-received as well as the deformed (ratcheted) stainless steel is shown in Fig. 4.3 It is evident from the figure that the investigated X12CrMnNiN17-7-5 stainless steel is completely austenitic in as-received condition exhibiting peaks corresponding to austenite (γ) only.

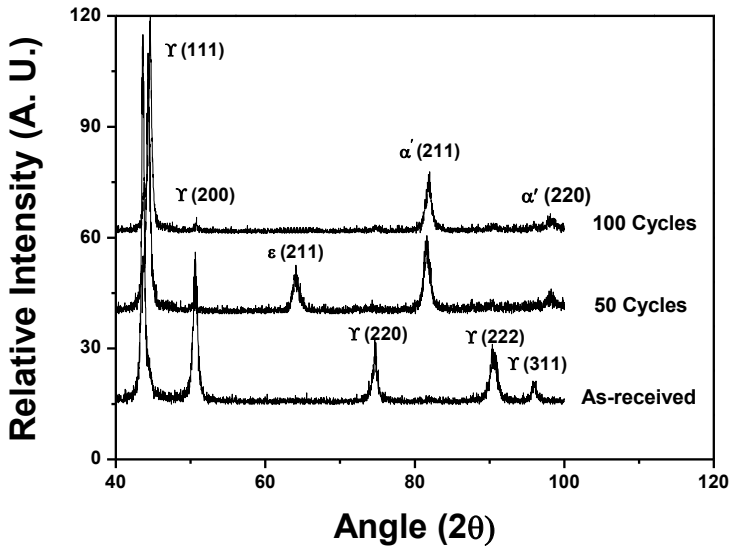

Fig. 4.3: XRD patterns obtained from the as-received as well as the ratcheted specimens subjected to 50 and 100 cycles of loading.

The pattern of the specimen subjected to ratcheting up to 50 cycles exhibits peaks corresponding to austenite (γ, FCC), ε-martensite (HCP) and α´-martensite (BCC) whereas the specimen subjected to 100 cycles exhibit peaks corresponding to austenite and α´-martensite only. Thus, following deformation a partial transformation from austenitic to martensitic phase took place. The present observation is consistent with the reported literature that during initial stages of deformation, austenite transforms into hexagonal close packed ε-martensite and on further deformation this ε-martensite transforms to body centered cubic α´-martensite [24]. A complete set of fatigue experiments in the present investigation were carried out up to some intermediate number of cycles i.e., 50 cycles. Therefore, the deformation introduced in the specimens was not significant and accordingly, the ε-martensite remains present in the specimens. The specimens

subjected to ratcheting deformation up to 100 cycles resulted austenite and α´-martensite indicating that the martensite transformation is complete.

4.4. Estimation of dislocation density in the ratcheted specimens

The modified Williamson–Hall equation [17] is employed in order to calculate the dislocation densities in the austenite (γ) and martensite (α´) phases in the stainless steel under investigation at room temperature. Assuming that the strain broadening is caused owing to the presence of the dislocations generated during the ratcheting deformation, the full width at half maximum (FWHM) of diffraction profiles can be expressed by the modified Williamson–Hall plot as [17]

$$\Delta K \cong 1/d + \left(\frac{\pi M^2 b^2}{2}\right)\rho^{1/2}\left(K^2\overline{C}\right) + O\left(K^4\overline{C}^2\right) \quad \text{……..(1)}$$

where $K = 2\sin\theta/\lambda$, $\Delta K = \cos\theta(\Delta 2\theta)/\lambda$, θ is the diffraction angle, Δ(2θ) is the integral breadth (FWHM) of the diffraction peak, λ is the wavelength of the X-rays, d is the average grain size, b is the length of the Burgers vector of the dislocations and ρ is the average dislocation density. M is a constant depending on both the effective outer cut-off radius of dislocations and the dislocation density. The value of M varies in between 1 and 2 for deformed materials [18,19]. Following this proposition, the value of M = 2 is used for all the specimens subjected to ratcheting deformation in the present investigation. The value of C represents the average contrast factor of the dislocations for a particular reflection. The average contrast factor for different diffraction vectors are defined as:

$$C = C_{h00}\left[1 - q\left(\frac{h^2k^2 + k^2l^2 + l^2h^2}{h^2 + k^2 + l^2}\right)\right] \quad \text{……..(2)}$$

where C_{h00} is the average contrast factor corresponding to h00 reflection. The value of C_{h00} = 0.266 is obtained from Ungár et al. [20]. The value of q = 2.203 is calculated based on the expression provided in Ungár et al. [20]. O indicates non-interpreted higher order terms in $K^4\overline{C}^2$ and therefore, the term containing it is ignored in equation (1). The X-ray diffraction profiles used for the analysis were (111), (200), (220) and (311) corresponding to γ phase and (110), (200), (211), (220) and (310) corresponding to α′ phase. The full width at half maximum (FWHM) and the diffraction angle of all the peaks were obtained and used for the subsequent analyses. The magnitudes of the Burgers vectors of the γ (= 0.254 nm) and α′(= 0.252 nm) phases were calculated from the respective lattice constants as well as elastic constants of austenitic steel. An average value of b = 0.253 nm is used for all calculations.

The ΔK for each (hkl) peak is plotted as a function of K^2C following the modified Williamson–Hall equation and is shown in Fig. 4.4 (a&b) for the specimens subjected to ratcheting deformation up to 50 and 100 cycles, respectively. A separate plot is shown corresponding to 50 as well as 100 cycles for obtaining better clarity exhibited by the fitted lines. It is evident from the plots that good fits are obtained for all the curves. The modified Williamson–Hall plot provides two important microstructural features.

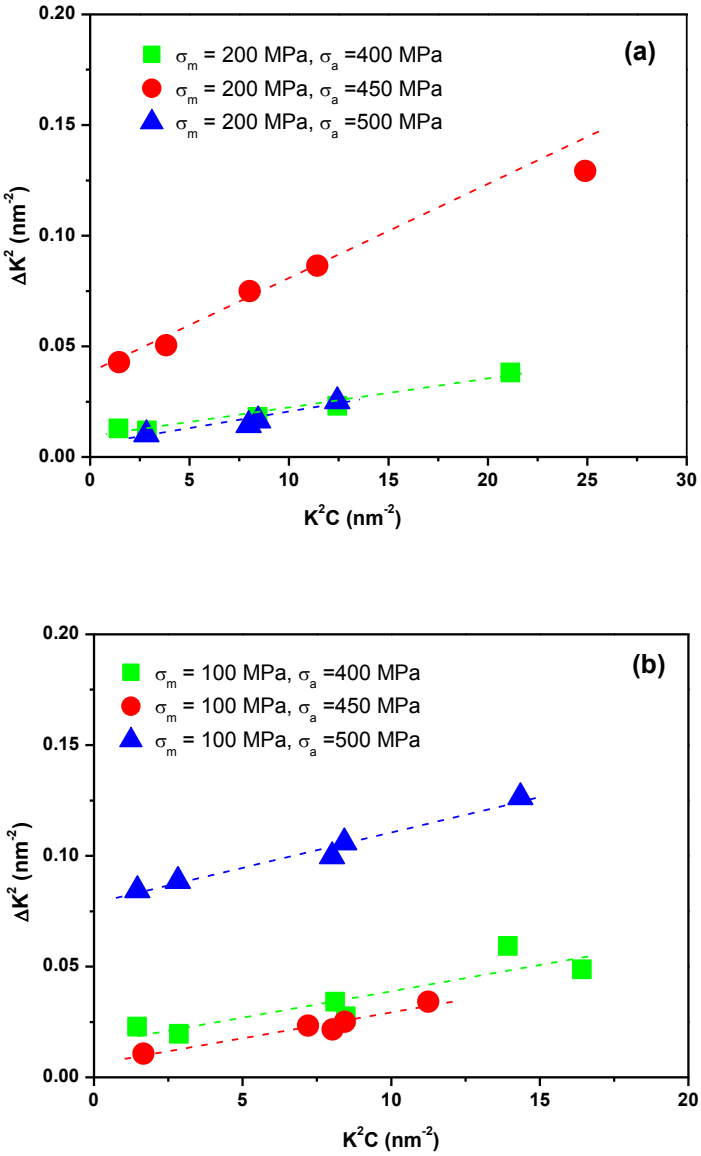

Fig. 4.4: Peak broadening analysis using the modified Williamson-Hall plot.

The intersection at K = 0 of the linear fit of the curves provide the average grain size (1/d) or the diffraction domain size. The slope (m) of the fitted curve is used to calculate the dislocation density from the following equation

$$\rho = \frac{2m^2}{\pi M^2 b^2} \quad \ldots\ldots\ldots\ldots\ldots (3)$$

where m is the slope of the linear fit of the data points on the ΔK vs. K^2C plot.

The dislocation densities in the ratcheted specimens calculated following the modified Williamson–Hall equation is included in Fig. 4.5(a&b) as well to establish the relationship between the dislocation densities and the corresponding ratcheting strain with varying mean stresses (σ_m), stress amplitudes (σ_a) and number of cycles (N). It is evident from the figures that the calculated dislocation densities for all the specimens increase with increase in ratcheting strain, as expected. The dislocation density generally increases significantly when stainless steels undergo martensitic transformation following deformation [25,26]. The accumulation of ratcheting strain and accordingly, the dislocation density increases with mean stress at constant stress amplitude (σ_a) and number of cycles (N). However, the increase in dislocation density is very prominent with increase in stress amplitude and a dislocation density of 8.131×10^{15} m^{-2} corresponding to the ratcheting strain of 0.4620 is obtained. Similarly, the dislocation density increases with increase in stress amplitude (σ_a) at constant mean stress (σ_m) and number of cycles

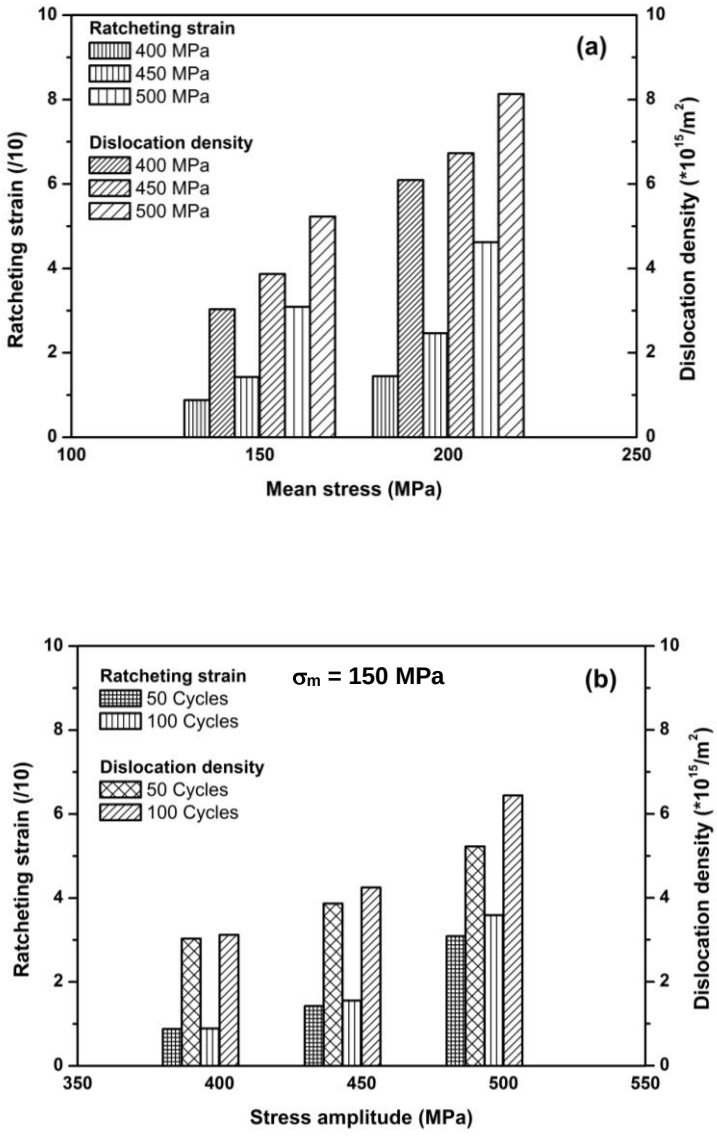

Fig. 4.5: Variation of ratcheting strain and dislocation densities with (a) varying mean stresses of 150 and 200 MPa, at constant stress amplitudes; (b) varying stress amplitudes at constant mean stress of 150 MPa for 50 and 100 cycles.

(N), and a value of 6.44×10^{15} m^{-2} corresponding to the ratcheting strain of 0.3590 is obtained. For comparison, the dislocation density was estimated following the same method in the as-received steel as well and was found to be 1.825×10^{14} m^{-2}. It is evident that the dislocation densities in the ratcheted specimens have increased by almost an order of magnitude. The difference in the accumulation of ratcheting strain corresponding to 50 as well as 100 cycles at a constant mean stress (σ_m) and stress amplitude (σ_a) is not very significant, as can be observed in Fig. 4.5(b). The present observation is consistent with the reported observation that the accumulation of ratcheting strain attains a saturation plateau after about 100 cycles of loading for stainless steels. In general, during ratcheting deformation two synergistic features i.e., variation of dislocation densities and martensitic transformation take place and these depend on the extent of fatigue damage induced in the investigated steel.

4.5 Separate calculation of dislocation density for different phases and dislocation character of each phase:

In the above calculation dislocation density measured was an average value and it was independent of phase changes but in real there are some dependencies of dislocation on phase changes.

4.5.1 Estimation of screw and edge dislocation density in the ratcheted specimens:

In the present work, individual contrast factors for face centred cubic (FCC) and body centred cubic (BCC) are compiled for probable directions as a link of elastic constant. There will be some changes in the value of $\bar{C}_{h00}$ and a new parameter q will be introduced for the separate calculation of edge and screw dislocation in FCC and BCC phase.

4.5.1.1 The value of $\bar{C}_{h00}$ in FCC and BCC crystals:

Calculation of average values of the contrast factors were done for the most common slip systems in the FCC and BCC systems. Value of $\bar{C}_{h00}$ in both cases like edge and screw were evaluated by arithmetic averages of the individual C_{h00} values and these are the functions of A_i and C_{12}/C_{44}. No dependence on c_{12}/c_{44} was seen for screw dislocations in case of f.c.c. crystals, while in case of edge dislocations, a comparatively strong dependence on c_{12}/c_{44} was observed. The A_i dependence of $\bar{C}_{h00}$ at different c_{12}/c_{44} values can be parameterized by the following function:

$$\bar{C} = a[1-\exp(-A_i/b)] + cA_i + d \ldots\ldots\ldots (4)$$

The corresponding values of a,b,c,d for FCC as well as BCC are listed in table 4.2.

4.5.1.2 The values of q in FCC and BCC crystals:

In the range between 0.5 and 3 q is found to be independent of C_{12}/C_{44} for screw dislocations (at least in f.c.c. crystals). In case of edge dislocations, q shows a weak dependency on C_{12}/C_{44} in the range of 0.5 to 1, while in between 1 and 3 this dependency becomes trivial. The A_i dependence of q at different c_{12}/c_{44} values can be characterized by the same kind of equation as

$$q = a[1-\exp(-A_i/b)] + cA_i + d \ldots\ldots\ldots (5)$$

The values of a, b, c, d for FCC as well as BCC are listed in Table4.3. Large difference can be found, especially in the range of 0.5 and 4 for A_i. For screw dislocations, a feeble dependency onC_{12}/C_{44} can be seen. For edge dislocations, the dependency on C_{12}/C_{44} is relatively stronger**.**

Table 4.2 Value of a,b,c,d for $\overline{C}$ in FCC and BCC phase.

FCC			BCC		
	Edge dislocation	Screw dislocation		Edge dislocation	Screw dislocation
a	0.1687	0.1740	a	1.6690	0.1740
b	2.0400	1.9522	b	21.124	1.9522
c	0.0194	0.0293	c	0.00	0.0293
d	0.0926	0.0662	d	0.0757	0.0662

	FCC	FCC		BCC	BCC
	Edge dislocation	Screw dislocation		Edge dislocation	Screw dislocation
a	4.8608	5.4252	a	7.2361	8.6590
b	0.8687	0.7196	b	0.9285	0.3730
c	0.0896	0.0690	c	0.1359	0.0422
D	-3.4280	-3.1970	d	-5.7484	-6.074

Table4.3 Value of a,b,c,d for q in FCC and BCC phase.

4.5.1.3 Evaluation of dislocation character:

The ΔK vs $KC^{1/2}$ is plotted as a function of modified Williamson–Hall equation and is shown in Fig. 4.6 & Fig.4.7 for the specimens having BCC and FCC phase, respectively. A separate plot is shown for edge and screw dislocation with ratcheting strain for BCC and FCC both phases in Fig.4.8 & Fig.4.9. It is evident from the plots that good fits are obtained for all the curves.

And also it can be seen from the figures that the dislocation density continuously decreases in case of edge dislocation in FCC and increases in BCC and for screw dislocation there is increment in dislocation density for both the phases.

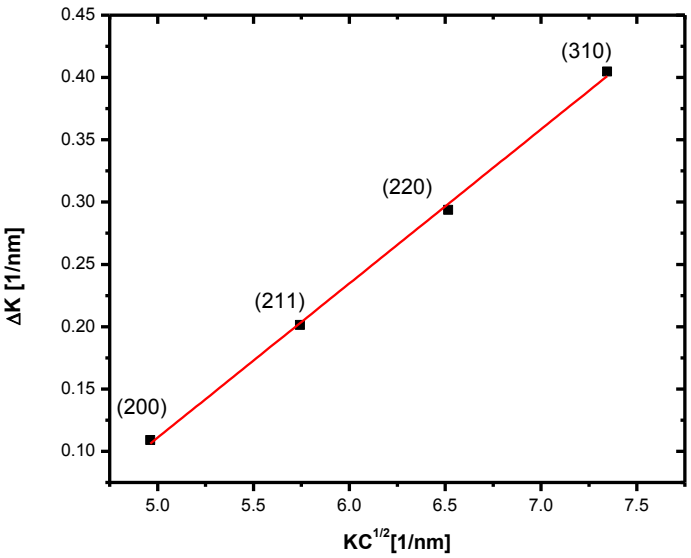

Fig.4.6 Value of FWHM according to modified Williamson- Hall plot for BCC.

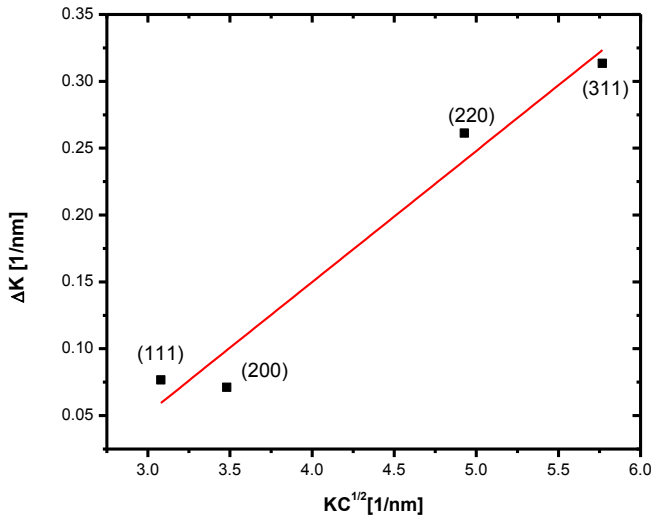

Fig.4.7 Value of FWHM according to modified Williamson- Hall plot for FCC.

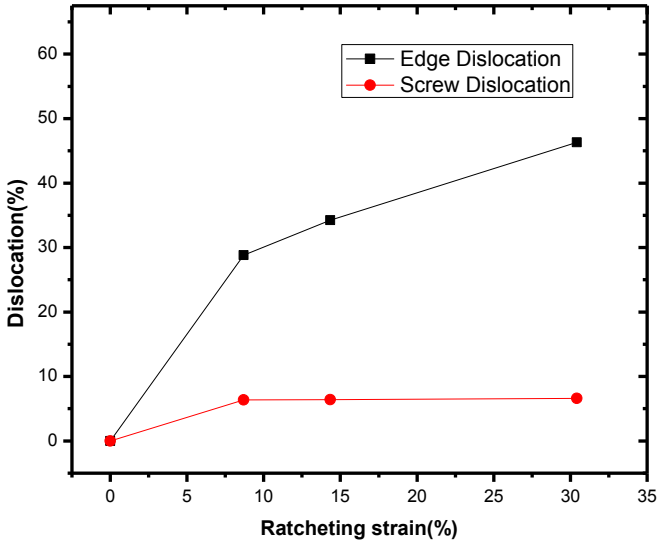

Fig.4.8 The edge/screw dislocation as a function of ratcheting strain for BCC.

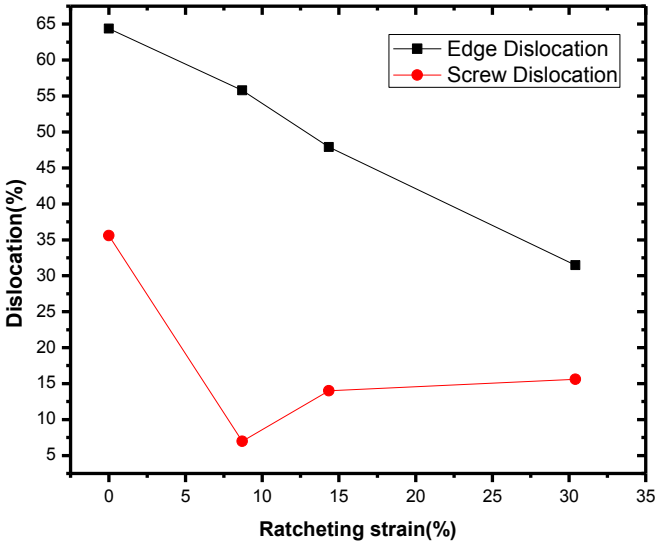

Fig.4.9 The edge/screw dislocation as a function of ratcheting strain for FCC.

A comparison graph is shown for all these changes in Fig.4.10 & Fig.4.11. With the help of this graph it can be seen that edge dislocation decreases while screw dislocation increases for 50 as well as 100 cycles.

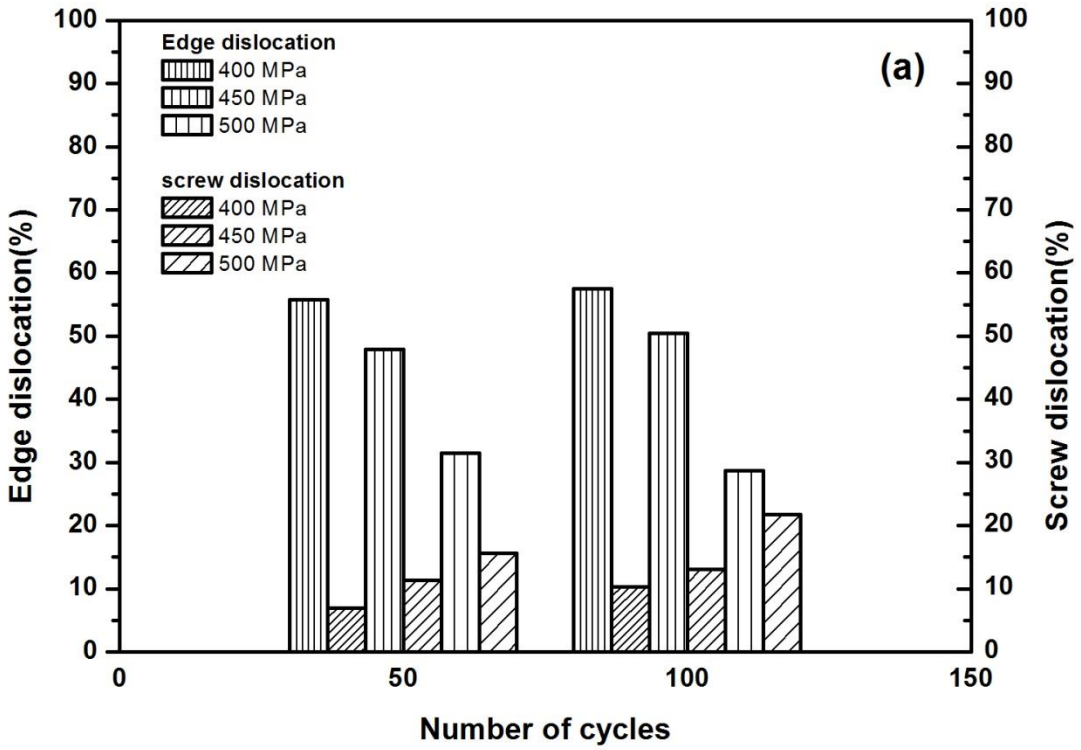

Fig.4.10 Variation in edge and screw dislocation with number of cycles.

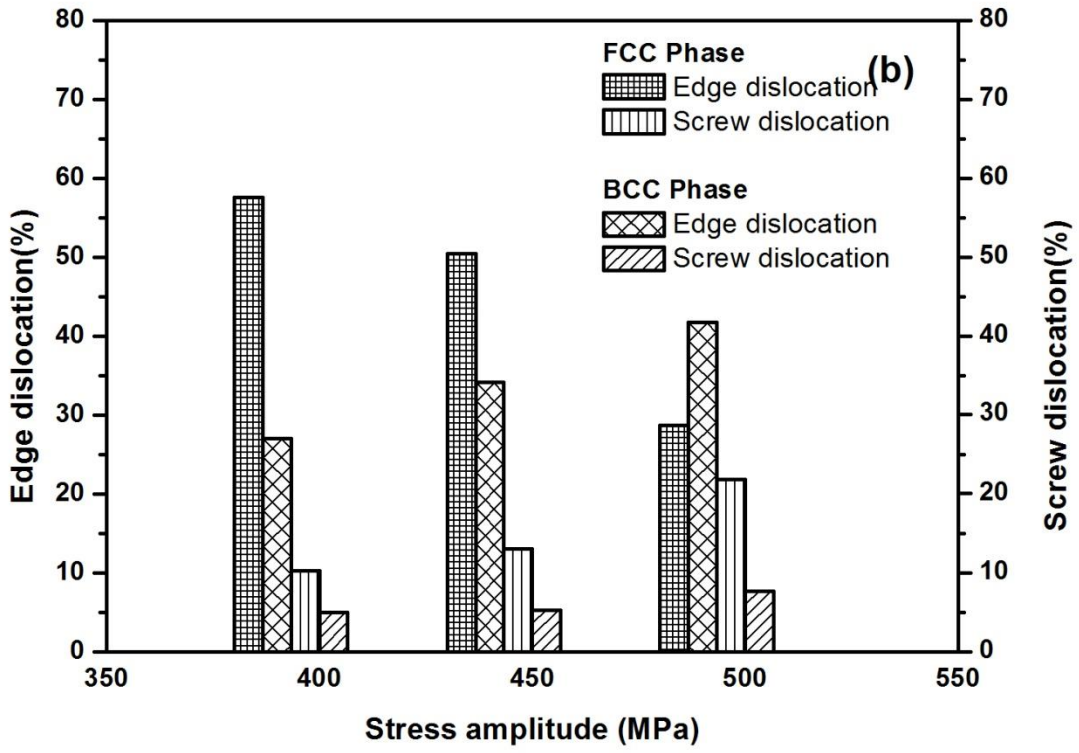

Fig.4.11 Variation in edge and screw dislocation with stress amplitude.

While comparing dislocation density with varying stress amplitude it can be seen that edge dislocation for FCC goes on decreasing while screw dislocation increases with increasing stress amplitude from 400Mpa to 500Mpa but in case of BCC both edge and screw dislocation increases with increasing stress amplitude.

CHAPTER 5

CONCLUSIONS

5.1 Conclusions:

Asymmetric stress-controlled fatigue (ratcheting) behaviour of a non-conventional stainless steel has been investigated with varying mean stresses, stress amplitudes and number of cycles. The X-ray diffraction profile analysis using the modified Williamson–Hall equation has been carried out in order to estimate the dislocation densities in the specimens subjected to ratcheting deformation and a correlation between the strain produced by ratcheting and the estimated dislocation density has been established. The following conclusions can be drawn in the light of the present investigation:

1. The X-ray diffraction profile analysis can successfully be employed to estimate the dislocation density in the investigated non-conventional stainless steel subjected to ratcheting deformation. The calculated dislocation densities of all the specimens increase with increase in ratcheting strain and the values were almost an order of magnitude higher than that obtained in the as-received steel.
2. The accumulation of ratcheting strain and accordingly, the dislocation density increases with mean stress at constant stress amplitude and number of cycles. It was observed that the dislocation density increases from 3.03×10^{15} m^{-2} to 6.09×10^{15} m^{-2} with increase in ratcheting strain from 0.088 (σ_m = 150 MPa) to 0.145 (σ_m = 200 MPa).
3. The dislocation density increases with increase in stress amplitude at constant mean stress and number of cycles. For example, when ratcheting strain increases from 0.088 (σ_a = 400 MPa) to 0.309 (σ_a = 500 MPa) the dislocation densities increases from 3.03×10^{15} m^{-2} to 5.23×10^{15} m^{-2}.

4. In line with natural expectation, the investigated non-conventional stainless steel undergone deformation induced martensitic transformation, which is also responsible for increasing dislocation densities affecting ratcheting behavior of the investigated steel.
5. In FCC with constant mean stress and increasing stress amplitude edge dislocation percentage goes on decreasing while screw dislocation percentage goes on increasing while in BCC edge and screw both dislocation percentage goes on increasing.
6. In both the phases there is edge as well as screw dislocation. Out of these two edge dislocation is more dominant in both phases.

References:

[1] J. R. Davis (Ed.), ASM Specialty handbook - Stainless steels, ASM International, USA, 1999.

[2] A.K. De, D.C. Murdock, M.C. Mataya, J.G. Speer, D.K. Matlock, Scripta Mater. 50 (2004) 1445–1449.

[3] J. Talonen, P. Nenonen, G. Pape, H. Hanninen, Metal. Mater. Trans. A 36 (2005) 421–432.

[4] M.A. Krivoglaz, Theory of X-ray and Thermal Neutron Scattering by Real Crystals, Plenum Press, New York, 1996.

[5] J. Gubicza, G. Ribárik, G.R. Goren-Muginstein, A.R. Rosen, T. Ungár, Mater. Sci. Eng. A 309–310 (2001) 60–63.

[6] G. Faraji, M.M. Mashhadi, A.R. Bushroa, A. Babaei, Mater. Sci. Eng. A 563 (2013) 193–198.

[7] T. Shintani, Y. Murata, Acta Mater. 59 (2011) 4314–4322.

[8] J. Gubicza, J. Szepvolgyi, I. Mohai, L. Zsoldos, T. Ungar, Mater. Sci. Eng. A 280 (2000) 263–269.

[9] T. Ungár, G. Ribarik , L. Balogh, A.A. Salem, S.L. Semiatin, G.B.M. Vaughan, Scripta Mater. 63 (2010) 69–72.

[10] M.J. Hordon, B.L. Averbach, Acta Metal. 9 (1961) 247–249.

[11] http://en.wikipedia.org/wiki/Stainless_steel last accessed on 16th May 2014.

[12] http://en.wikipedia.org/wiki/Fatigue_(material) last accessed on 16th May 2014.

[13] Ringsberg, J. W. (2001), Life prediction of rolling contact fatigue crack initiation, International Journal of Fatigue, Vol. 23, pp. 575–586.

[14] Satyadevi, A., Sivakumar, S.M. and Bhattacharya, S.S. (2007), A new failure criterion for materials exhibiting ratcheting during very low cycle fatigue, Materials Science and Engineering A, Vol. 452-453, pp. 380–385.

[15] http://en.wikipedia.org/wiki/Dislocation last accessed on 19th May 2014

[16] A. Nayar, The Steel Handbook, Mc Graw Hill Education, UK, 2001, 829–832.

[17] T. Ungár, A. Borbély, Appl. Phys. Let. 69 (1996) 3173–3175.

[18] T. Ungár, Mater. Sci. Eng. A 309–310 (2001) 14–22.

[19] G. Ribarik, T. Ungár, Mater. Sci. Eng. A 528 (2010) 112–121.

[20] R.A. Renzetti, H.R.Z. Sandim, R.E. Bolmaro, P.A. Suzuki, A. Moslang, Mater. Sci. Eng. A 534 (2012) 142–146.

[21] K.K. Ray, K. Dutta, S. Sivaprasad, S. Tarafder, Procedia Eng. 2 (2010) 1805–1813.

[22] K. Dutta, S. Sivaprasad, S. Tarafder, K.K. Ray, Mater. Sci. Eng. A 527 (2010) 7571–7579.

[23] K.K. Ray, H. Roy, A. Ray, K. Dutta, S. Tarafder, Adv. Mater. Res. 794 (2013) 415–428.

[24] H. Roy, A. Ray, K. Barat, C. Hochmuth, S. Sivaprasad, S. Tarafder, U. Glatzel, K.K. Ray, Mater. Sci. Eng. A 561 (2013) 88–89.

[25] M. Tokizane, N. Matsumura, K. Tsuzaki, T. Maki, I. Tamura, Metal. Trans. A 13 (1982) 1379–1388.

[26] M. Kehoe, P.M. Kelly, Scripta Metal. 4 (1970) 473–476.